Structure–property relationships in styrene–butyl acrylate emulsion copolymers: 2. Viscoelastic properties of latex films—experimental results and simulation

B. Schlund, J. Guillot and C. Pichot*
LMO–CNRS, BP 24, 69390 Vernaison, France

and A. Cruz
Facultad de Quimica, UNAM, 04510 Mexico DF, Mexico
(Received 11 October 1988; revised 18 May 1989; accepted 23 May 1989)

Dynamic mechanical properties as a function of temperature (−100 to 130°C) have been investigated on films made from styrene–butyl acrylate copolymer latexes prepared by emulsion polymerization using three different processes and various comonomer compositions (25/75, 50/50, 75/25) so as to obtain different particle morphologies. With the homogeneous copolymers, it was found that the variation of the viscoelastic properties vs. the composition can be modelled with a linear law, which shows the similarity, at a molecular level, between a two-phase composite and a homogeneous copolymer. In the case of core–shell or multilayered latex particles, thermomechanical analysis of the corresponding films suggests that two or three phases exist; the nature and the composition of the matrix and inclusion phases were deduced from the simulation of the experimental data using a self-consistent composite model based on Kerner's equation adpated by Dickie for a strain model.

(Keywords: styrene; butyl acrylate latexes; particle structure; film morphology; microstructure; dynamic mechanical properties; simulation)

INTRODUCTION

In the last decade, many fundamental studies have been devoted to polymer alloys, a class of materials that has been increasingly attractive because of interest in industrial applications. Now, many processes, related to adapted characterization methods, allow one to prepare polymer composites at a very low size level (~10 Å), such as the microcomposites that originate from block copolymers or semicrystalline polymers.

Among these processes, emulsion polymerization is currently carried out for the synthesis of heterogeneous materials. The development of new controlled processes (multistage polymerization, corrected or composition-gradient, batch or semi-batch, etc.) is particularly useful to obtain composite particles having core–shell, multilayer or homogeneous structures[1]. Coalescence of these model latexes was found to provide heterophase films, with a morphology well defined from dynamic mechanical spectroscopy and adapted theoretical equations. The present work aims at giving recent results obtained in this domain.

The analytical determination of the properties of a multiphase system from the properties of each constituent phase is not really new, Hashin[2] and Nielsen[3] having reviewed in detail such a challenge. The theoretical issue is quite complex since it is necessary to account for physical parameters (geometry, morphology, interfacial zone) that are more typical of the composite itself than of the constituent phases; as a result, well defined structure models are required. A self-consistent model was selected: it does not allow access to all the physical parameters of the composite. However, when applied to simple structured particles, comparison of experimental and simulated results gives information on phenomena arising during film formation and phase rearrangement as a function of temperature.

Experimental results were obtained from the thermomechanical properties of films cast by the coalescence of styrene (S)–butyl acrylate (BuA) latexes with various overall compositions (S/BuA in mol%: 25/75, 50/50, 75/25) and exhibiting different particle morphologies (homogeneous, core–shell (PS (I)/BuA–S (II)) and multilayer (PS (I)/BuA–S (II)/PBuA (III)). The preparation and characterization of these latexes have already been described in a companion paper[4].

THEORETICAL REVIEW

It has long been recognized that the properties of a composite can be determined from the properties of the constituent phases, their geometric shape and the nature of the interface between the phases. Most expressions describing the viscoelastic behaviour of such heterophase systems are derived from viscosity theories applied to suspensions[5]. The analogy between viscosity and shear moduli in solid-state measurements leads to the substitution of the shear ratio in a viscosity relationship by the strain ratio in a modulus equation.

For instance, a composite system formed with an elastomer matrix (Poisson ratio $\nu = 0.5$) and rigid inclusions will obey the following equation between

* To whom correspondence should be addressed

0032-3861/89/101883-12$03.00

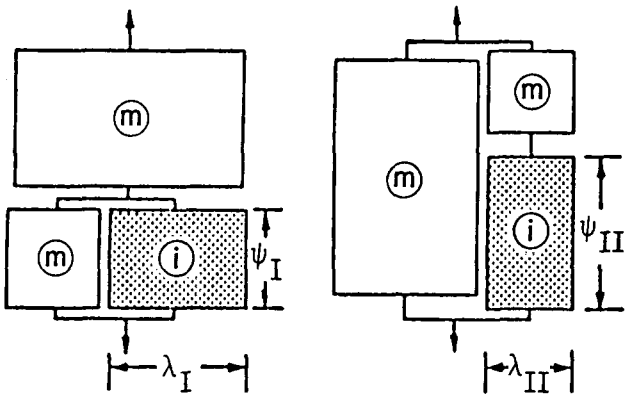

Figure 1 Takayanagi's model (m, matrix phase; i, inclusion phage). λ_I, λ_{II}, ψ_I, ψ_{II} are fitting parameters for modelling the behaviour either in series or in parallel. $\lambda_I\psi_I=\lambda_{II}\psi_{II}=v_i$

viscosity and moduli:

$$\eta/\eta_m=G/G_m \tag{1}$$

where η is the dynamic viscosity (Pa s), G is the shear modulus (Pa) and subscript m denotes the matrix phase. Nielsen[6] proposed a more general equation, which introduces the Poisson ratio (v) of the matrix and inclusions:

$$\left(\frac{\eta}{\eta_m}-1\right)=\frac{2.5(8-10v_m)}{15(1-v_m)}\left(\frac{G}{G_m}-1\right) \tag{2}$$

with η, G and m having the same meanings as previously.

The theoretical expressions that relate the structure or morphology parameters of the system to the mechanical properties need to select models that account for the assumptions and the theoretical approach. Three main groups of models can be distinguished; all of them allow one to describe the modulus dependence upon the composition. The corresponding equations contain the moduli and Poisson ratios of the constituent phases and take into account a geometry factor and the degree of homogeneity of the dispersed phase. Some models consider the possibility of sliding at the interfaces or also suggest the existence of interphases[7]. Takayanagi *et al.*'s work[8] is an illustration of the first group: the viscoelastic properties of the composite are represented in terms of simple mechanical models comprising elements (supposed to exhibit the viscoelastic properties of the constituent phases) that are partly connected either in series or in parallel. A number of other authors[9–12] successfully used this approach. *Figure 1* describes such models of associations, which are mechanically equivalent[13]. Dickie[13] proposed a modified but interesting expression, which uses only one coupling parameter:

$$\frac{G_c}{G_m}=\frac{v_mG_m+(\alpha+v_i)G_i}{(1+\alpha v_i)G_m+\alpha v_mG_i} \tag{3}$$

where G is the shear modulus, v is the volume concentration of a component phase, subscripts c, m, i relate respectively to the composite, the matrix and the inclusions, and α is a coupling factor related to the parameters λ_I, ψ_I, λ_{II}, ψ_{II} defined on *Figure 1* by the following equations:

$$\lambda_I=v_i/\psi_I=(\alpha+v_i)(1+\alpha)$$
$$\lambda_{II}=v_i/\psi_{II}=v_i(1+\alpha)/(1+\alpha v_i)$$

Here λ and ψ are respectively parameters that determine the range of the series and parallel associations for the two phases.

Although these models have been extended[14,15] or generalized[16,17] they only offer a phenomenological aspect of the mechanical behaviour and not a physical view of the structure.

The second type of model, called 'self-consistent models', is based on an idealized picture of the structure (*Figure 2*): the polymer forming the inclusion (i) is occluded in a composite sphere comprising the polymer forming the matrix (m, inner layer) and the composite (c, outer layer). Kerner[18] first used this approach and obtained the relationship (4) between the shear moduli. Dickie[13] demonstrated that the same expression (4) could be available for the complex Young's modulus:

$$\frac{G_c}{G_m}=\frac{v_mG_m+(\beta+v_i)G_i}{(1+\beta v_i)G_m+\beta v_mG_i} \tag{4}$$

with

$$\beta=2(4-5v_m)/(7-5v_m)$$

and v_i, G, m and i as already mentioned. In these calculations Kerner chose $(r_i/r_m)^3=v_i$ (see the definition in *Figure 2*); a better agreement with the experimental results was obtained by modifying the ratio $(r_i/r_m)^3$ (ref. 19). Nielsen[20] and Dickie[21] proposed an effective volume fraction v_{eff} such as

$$v_{eff}=v_i+v_i^2(1-v_{im})/v_{im}^2 \tag{5}$$

where v_{im} is a fitting factor so as to obtain a better agreement between the experimental and simulated results. For hard-sphere inclusions in a soft matrix, $0.6<v_{im}<0.65$, and for soft particles in a rigid matrix, $<0.8<v_{im}<0.83$.

Based on the same model, Halpin[22] and Tsai[7] established a more general relationship, which takes into account the degree of homogeneity (packing factor, v_i), the shape of inclusions and the type of stress. From simple assumptions, this approach allows one to give an approximate description of the modulus behaviour as a function of conversion; hence many authors used it[13,23].

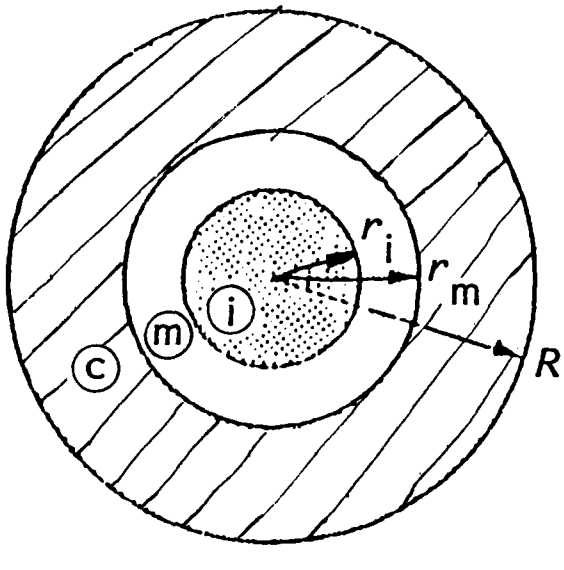

Figure 2 Model structure of Kerner, the self-consistent model (m, matrix; i, inclusion; c, composite). $v_i=(r_i/r_m)^3$

The third type of model consists of determining the minimum and maximum limits of the composite modulus from general considerations and assumptions such as the energy of minimal strain. The computations of Paul[24], Hashin[25] and Strikman[26] show that it is possible, without any hypothesis on the morphology, to determine the range of values for the composite modulus. The analytic expression can be reduced to the more simple ones of Kerner if the matrix and inclusion are defined. However, such a model is able to show if: (i) the composite is homogeneous (ii) the mechanical behaviour of the constituent phases is the same in the pure state as in the mixture; and (iii) there is perfect adhesion between the phases.

Dickie[13,21] proved that these models were mathematically equivalent. Christensen[27] showed that such equations, originally established for describing the static elastic modulus behaviour, are also applicable to the viscoelastic complex modulus. One only needs to use the principle of equivalence between elastic and complex moduli and to derive the mathematical expressions of the real and imaginary components of the modulus in the case of a dynamic stress[26,27]. The substitution of G^* by G in equation (4) involves $v^*=v'+iv''=v'=$ constant, which is theoretically not correct. However, Dickie[13], starting from the study of Theocaris[28], showed that v'' could be neglected. Then, equation (4) for a dynamic stress is as follows:

$$\frac{E^*}{E_m^*}=\frac{[(1-v_i)E_m^*+\beta(\alpha+v_i)E_i^*]\gamma}{(1+\alpha v_i)E_m^*+\alpha\beta(1-v_i)E_i^*} \qquad (6)$$

with

$$\beta=(1+v_m)/(1+v_i)$$

and

$$\gamma=(1+\alpha)/(1+v_m)$$

MODELLING

The purpose was not to build up and to apply a theoretical model but rather to use a simple and sufficiently precise mathematical tool, so as to provide information on the latex film morphology: matrix/inclusion system in a continuous medium, nature of the phases, existence of an interphase.

The 'self-consistent' model of Kerner[18], Dickie[13] and Diamant[23] was chosen. As demonstrated by Hashin[2], this approach is not rigorous enough since microvariables are postulated to be equivalent to macrovariables (scaling phenomena?). The various expressions proposed by Kerner[18], Dickie[13] or Nielsen[6] for computing the complex modulus variation as a function of the temperature assume that thermal expansion effects can be neglected and that the initial established hypotheses are not temperature-dependent. On the contrary, a variation of the Poisson ratio *versus* temperature was admitted and an arbitrary law has been chosen, such as:

$v(T)=0.35$ before the T_g transition

$v(T)=0.5$ after the T_g transition

$v(T)\propto T$ in the T_g domain

Concerning the v_i factor defined in equation (5) and initially justified, the results of Dickie and Diamant clearly showed that it can be seen as a fitting parameter between the experimental and simulated curves. In the actual approach, v_{im} is considered and postulated to be equal to 1 because (i) the objective was not to reach the best agreement between the experiment and the theory and (ii) it does not account for the morphological aspect of the material. In fact, this parameter, when used, allows one to be free of the apparent nonsense of a material comprising 99% of dispersed phase in 1% of matrix, which represents according to equation (5) ($v_m=0.6$) a composite formed of a soft matrix with 59.5% of hard inclusions.

Methodology

The computer simulation of the thermomechanical behaviour of the composite needs the properties of the constituent phases or interphases to be known. The determination of the storage and loss moduli was performed according to equation (6), applying the equivalence principle between the complex and elastic moduli. Such a calculation leads to:

$$\begin{aligned}E_c'=&[(ABE_m'^2+ACE_i'E_m'-ABE''^2-ACE'')(DE_m'+FE_i')\\&+(2ABE_m'E_m''+ACE_i''E_m'+ACE_i'E_m'')(DE_m''+FE_i'')]\\&\times[(DE_m'+FE_i')^2+(DE_m''+FE_i'')^2]^{-1}\\E_c''=&[2ABE_m'E_m''+ACE_i''E_m'+ACE_i'E_m'')(DE_m'+FE_i')\\&-(DE_m''+FE_i'')\\&\times(ABE_m'^2+ACE_i'E_m'-ABE_m''^2-ACE_i''E_m'']\\&\times[(DE_m'+FE_i')^2+(DE_m''+FE_i'')^2]^{-1}\end{aligned} \qquad (7)$$

$$\tan\delta_c=E_c''/E_c'$$

with

$A=(1+v)/(1+v_m)$

$B=1-v_i$

$C=[(1+v_m)/(1+v_i)][2v_i(4-5v_m)/(7-5v_m)+v_i]$

$D=1+2v_i(4-5v_m)/(7-5v_m)$

$F=[2v_i(4-5v_m)/(7-5v_m)][(1+v_m)/(1+v_i)](1-v_i)$

For a material composite in which a composition gradient prevails from the inclusion phase to the matrix phase, it is possible to simulate the properties by splitting the interphase into n layers whose properties are well known. A stepwise calculus was performed as follows: first, the properties of the inclusion surrounded by a layer of polymer are determined using equation (7) and assuming a 'simple' inclusion geometry; then, the values obtained are used considering a new adjacent layer of polymer; and so forth until the last layer corresponds to the matrix phase.

Note that this approach suffers because the dimensions of the composite medium, as defined in Kerner's model (*Figure 2*) by the radius R, are small; thus the law established for infinite R values[29] is far from applicable. Since it seems difficult to quantify the error, this type of splitting has only been used for small values of n (3 to 5); therefore the interpretation of the results will only be considered as semi-quantitative.

EXPERIMENTAL

Synthesis and characterization of latexes

Latexes were prepared by emulsion polymerization of styrene with n-butyl acrylate using three processes, which

Table 1 Composition and structure of S–BuA latexes

Particle morphology	Polymerization process	Composition (S/BuA) (molar ratio) Theoretical (overall)	Various phases (from ^{1}H n.m.r.)			Code
Homopolymer	Batch	100/0	–			PS
		0/100	–			PBuA
Homogeneous copolymers	Corrected batch	25/75	27/73			BC1
		50/50	49/51			BC2
		75/25	73/27			BC3
Core–shell	Semi-continuous on PS seed (10% by wt)		Core	Shell		
		25/75	100/0	27/73		CS1
		50/50	100/0	45/55		CS2
		75/25	100/0	67/33		CS3
Multilayered (S/Copol/BuA)	Semi-continuous on PS seed (10% by wt) with different monomer feeds		Core	Copolymer shell	Pure BuA shell	
		25/75	100/0	23/77	0/100	MC1
		50/50	100/0	51/49	0/100	MC2
		75/25	100/0	84/16	0/100	MC3

have been described in more detail elsewhere[4]: corrected batch process (homogeneous particles)[30,31] and staged polymerization onto a PS latex in one step (core–shell particles) or two steps (multilayered particles)[32–34]. Various S/BuA compositions have been selected: 25/75, 50/50, 75/25 (mol%) respectively. *Table 1* summarizes the composition of the different latexes and the expected morphologies together with the particle sizes and molecular weights.

Preparation of films

Films were prepared by casting of raw latexes in moulded aluminium sheets. Film was recovered by water evaporation at 40°C (for low-T_g polymer composite) and at 80°C for styrene-rich copolymers (75/25). Good quality of the film was controlled by a slow rate of drying and three weeks ageing. Polystyrene film was obtained by compression moulding for 5 min at 180°C.

Electron microscopy analysis

The morphology of films and latexes was examined by transmission electron microscopy using Philips EM30 or JEOL 200 equipment; a cold stage was necessary for low-T_g polymers. Ruthenium tetroxide, which was recently reported[35,36] to reveal specifically many polymer phases, was used at an exposure time of 60 min. Preparation of specimens was as follows: in the case of the latex (0.5% by weight), a drop of the emulsion was deposited on the 200 mesh grid (not made of steel), then partially absorbed so as to keep a very thin layer of liquid; in the case of films, microtomed sections were obtained at low temperature (−90°C).

Viscoelastic properties

Dynamic mechanical properties as a function of temperature (−100 to 130°C) were obtained using a Viscoelasticimeter MAKO 3 (from Metravib). The complex traction (Young's) modulus was determined from sinusoidal a.c. stress ε ($1\ \mu m < E < 0.1$ mm) at 7.8 Hz frequency. The temperature gradient in the oven was 2°C and the temperature scanning rate was approximately 2°C min^{-1}. Film specimens were about $1 \times 13 \times 25$ mm.

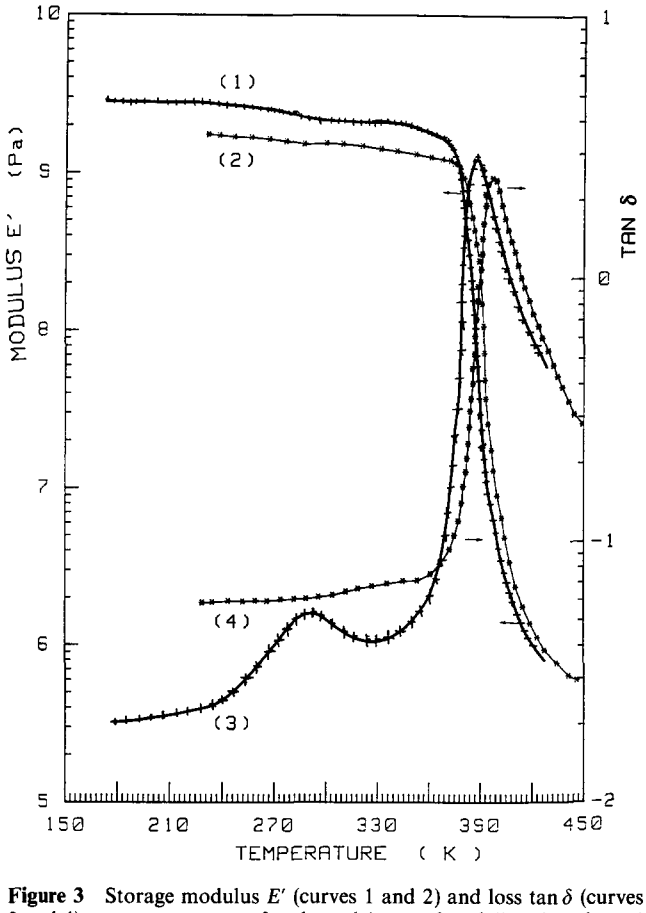

Figure 3 Storage modulus E' (curves 1 and 2) and loss tan δ (curves 3 and 4) *versus* temperature for cleaned (curves 2 and 4) and uncleaned (curves 1 and 3) polystyrene films

RESULTS AND DISCUSSION

Homogeneous copolymers

Effect of the emulsifier. Since the PS seed latex was obtained in the presence of approximately 4 g l^{-1} of emulsifier, a preliminary study was carried out in order to discriminate the influence of this ingredient, which represents 4% (in weight) in the final PS film. An emulsifier-free (clean) film was prepared after centrifuging (20 000 rpm for 3 h) the corresponding raw latex.

Figure 3 shows thermomechanical properties of films

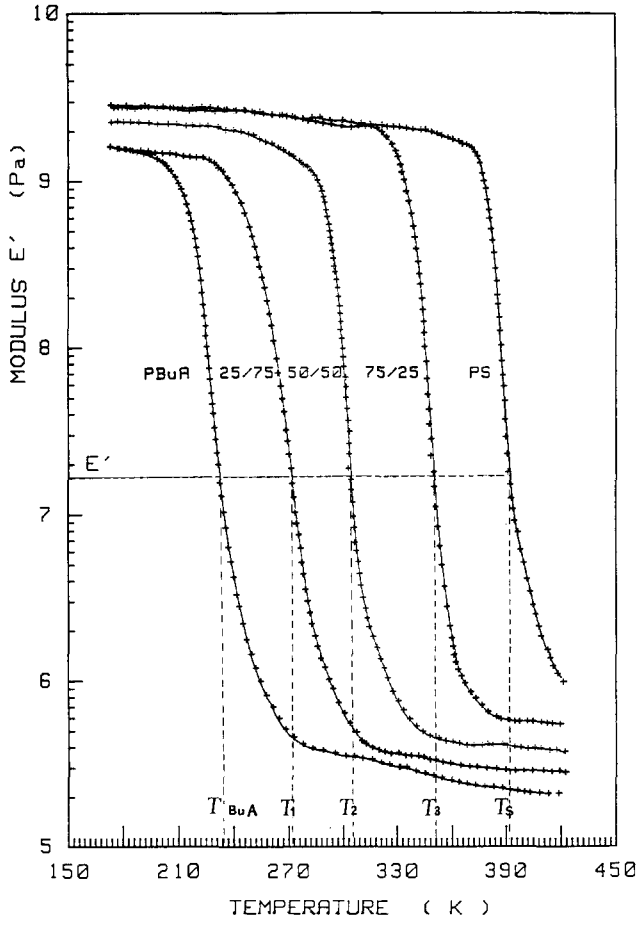

Figure 4 Comparison of storage modulus E' *versus* temperature for PBuA, PS and homogeneous copolymer films (respectively BC1, BC2 and BC3)

issued from clean and unclean (containing emulsifier) PS latexes. The damping peak (tan δ), located at 287 K, is assigned to the presence of the emulsifier; the magnitude of the peak suggests that the emulsifier forms a distinct phase in the material. The tan δ maximum at 390 K corresponding to the glass transition of the polymer is slightly shifted towards high temperatures when PS latex has been cleaned, which can reflect a plasticization effect of the polymer by the emulsifier. In the low-temperature range (-100 to -50°C) the experimental data (E' and tan δ) were not precise enough for discussions.

Effect of copolymer composition. Results on the dynamic behaviour as a function of temperature are shown on *Figures 4* and *5* for the three copolymers and both homopolymers. It is noteworthy that the different curves are regularly and similarly displaced along the temperature axis, which is representative of the good homogeneity of the material. An empirical linear transition rule was deduced between the temperature (T_x) for a given modulus (or tan δ) of a copolymer and its copolymer composition (x). If the curve $E'=f(T)$ (or $\tan\delta=f(T)$) for poly(butyl acrylate) is selected as the reference, this relationship is:

$$(T_x)_{E',\tan\delta}=(T_{BuA})_{E',\tan\delta}+(\bar{a})_{E',\tan\delta} \qquad (8)$$

where subscript E', tan δ means E' = constant and tan δ = constant, $(T_{BuA})_{E'}$ is the temperature for which the modulus is E' (with respect to the P(BuA) curve), x is the copolymer composition (molar fraction of S) and $\bar{a}$ is the 'mean' transition value from T_{BuA}.

In the present case, the $\bar{a}$ parameter was evaluated by cross-combination of the curves for the homopolymers and the three copolymers. It can be finally written as:

$$(\bar{a})_{E',\tan\delta}=(2T_{PS}-2T_{BuA}+1.4T_3+0.6T_2-0.2T_1)_{E',\tan\delta}$$

Subscripts 1, 2, 3 correspond to copolymers having composition (in mole ratio S/BuA) 25/75, 50/50, 75/25 respectively. This relationship has been applied for modelling the copolymer properties used in the synthesis of the structured particles.

In *Figure 4*, a difference is seen in the moduli at low temperature, the modulus corresponding to BC2 (50/50) being located between the two limiting ones relative to PS and PBuA. For any other composition, the modulus of the copolymer is near that of PBuA for the BC1 (25/75) sample or of PS for the BC3 (75/25) sample. No intermediate behaviour is observed between the composition 0–50% and 50–100%. The aforementioned difference in moduli for the two homopolymers at low temperature is explained[37] by the secondary transition of PBuA, which appears below -150°C.

Figure 5 exhibits the damping properties of the various copolymers as a function of temperature and the same procedure was applied for predicting the variation of tan δ vs. temperature as a function of the copolymer composition x.

Microstructure–property relationships. In a statistical copolymer, the sequence distribution can be easily

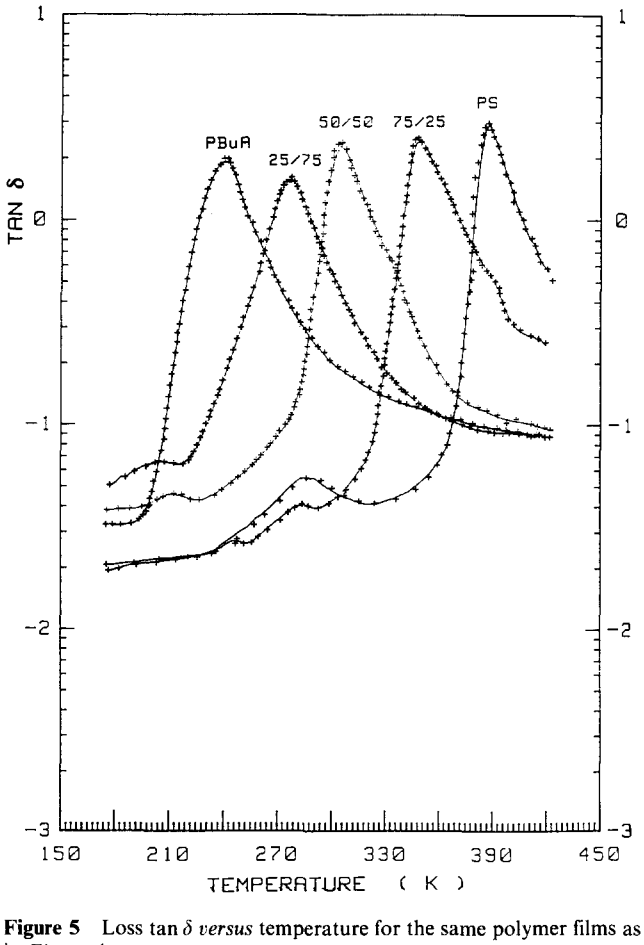

Figure 5 Loss tan δ *versus* temperature for the same polymer films as in *Figure 4*

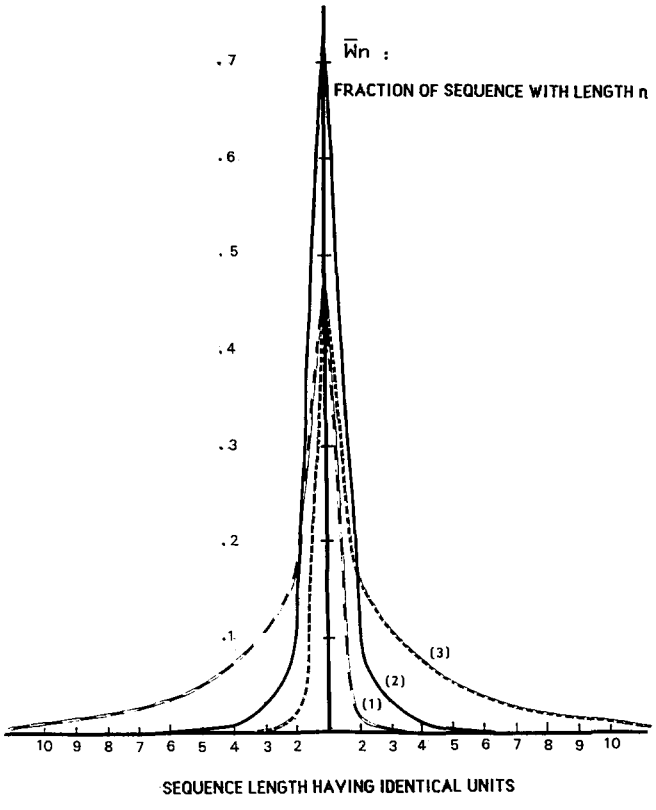

Figure 6 Fraction of monomer M_i engaged in sequences of length n, as a function of the number of monomer units in a given sequence, for copolymer compositions (molar ratio S/Bua): 25/75 (curve 1), 50/50 (curve 2) and 75/25 (curve 3)

calculated from the reactivity ratios and monomer feed composition within the polymer particles[38]. For the different dyads, it follows that:

$$\begin{aligned} AA &= PAA \times PBA/(PAB + PBA) \\ BB &= PBB \times PAB/(PAB + PBA) \\ (AB) &= (BA) = PAB \times PBA/(PAB + PBA) \end{aligned} \quad (9)$$

and for the triads:

$$AAA = (AA) \times PAA$$
$$BBB = (BB) \times PBB$$

with

$$PAB = 1/(1 + r_A[A]/[B]) \qquad PBA = 1/(1 + r_B[B]/[A])$$
$$PAA = 1 - PAB \qquad PBB = 1 - PBA$$

where r_A, r_B are the reactivity ratios for the A, B monomers and [A]/[B] represents the molar ratio of the monomer concentration at the polymerization locus. In the case of a corrected-batch process, this ratio has been calculated from the copolymerization equation:

$$n = dA/dB = (1 + r_A[A]/[B])/(1 + r_B[B]/[A]) \quad (10)$$

and it was kept constant for the duration of the polymerization.

Figure 6 gives an illustration of such a sequence distribution in S/BuA copolymers, $\bar{W}_n$ being the fraction of monomer M_i engaged in a sequence of length n composed of the same units M_i. These curves show that, for each composition, the peak distributions display a real asymmetry despite rigorous experimental conditions (control of the feed monomer composition). However, those distributions are actually relatively narrow for the copolymers with composition 25/75 or 75/25, since there is only less than 1% of sequences having 10 identical monomer units.

It is noteworthy to see that the $\tan\delta$ spectra (*Figure 5*) also exhibit the same but less pronounced asymmetry although the microstructure is practically homogeneous. This confirms, as recently underlined[39,40], that the chain microstructure plays a predominant role in the thermomechanical behaviour of copolymers (if the polymer material is amorphous).

Molecular approach to mechanical behaviour. In this part, it is attempted to show analogies between the behaviour of homogeneous copolymers with that of homopolymer mixtures. Let us consider, first, the minimum and maximum theoretical values of the modulus for a two-phase material constituted by a mixture of pure homopolymer phases, PS and PBuA. The maximum limit (Reuss limit) can be represented by the parallel-type association of phases, such as:

$$E_{c,\text{parallel}} = E_1 v_1 + E_2 v_2 = E_1[1 + (K-1)v_2] \quad (11)$$

with $K = E_2/E_1$ and v_1 and v_2 the volumes of PBuA and PS respectively.

A series-type association allows one to define the lower limit (Voigt limit) as:

$$1/E_{c,\text{series}} = \frac{v_1}{E_1} + \frac{v_2}{E_2}$$

or

$$E_{c,\text{series}} = \frac{KE_1}{K-(K-1)v_2} \quad (12)$$

It is found that the moduli for PS and PBuA are affected when varying the temperature; thus K is not a constant.

In order to examine the experimental results, not as a function of temperature (*Figures 4* and *5*) but as a function of the volume fraction of S, a three-dimensional description of the mechanical behaviour of the homogeneous copolymers is given in *Figure 7*, as a function of the modulus, temperature and composition.

Equations (11) and (12) are reported (broken curves) on *Figure 8* for three values of K (10, 10^2 and 10^3). Hence, the properties of the copolymer can be determined at various temperatures by varying the styrene volume fraction, and for different K values. Four values of K have been arbitrarily defined: 10, 10^2, 10^3 and 7×10^3. For each K value, two potential temperatures exist which are determined by the computer. The modulus values corresponding to these two temperatures have been reported in *Figure 8*, giving the variation $E'_{\text{copolymer}}/E'_{\text{PBuA}}$ *versus* mol% in the copolymer. This was performed for the different values of K and the corresponding curves are shown (full curves).

A detailed examination of *Figure 8* points out the analogy between the theoretical curves previously established and the experimental ones originating from the homogeneous copolymers. This analogy suggests that, at a molecular level, the homogeneous copolymer can be considered to be formed by pure homopolymer phases (S, BuA), each monomer unit exhibiting the property of the corresponding homopolymer. The main difference between the theoretical and experimental approaches is that, in the former one, covalent bonds are assumed.

Under Kerner's hypotheses, the inclusions and the matrix are totally connected, which suggests that there is no energy loss at the interface of the two constituents. In other words, it can be considered that the degree of binding between the phases is infinite in any given direction. In the case of a homogeneous copolymer material, the degree of binding for the monomer unit selected as inclusion is infinite in only the two directions defined by the covalent bonds; for the other direction, a certain freedom of motion can be allowed, which implies that a loss energy can occur during the transfer of strains in directions different from that defined by the covalent bonds.

Such an argument might explain the observed difference between the experimental and theoretical curves. For $K > 10^3$, one temperature only is found experimentally. An example is given in *Figure 8d*: for $K = 7 \times 10^3$, a maximum discrepancy is found between the PS and PBuA moduli. In this case, a mixed behaviour is noticed: for a BuA-rich composition the 'series'-type mechanical model seems well adapted whereas the 'parallel-type' model is more appropriate for S-rich composition. The transition between the two models, which is taking place at 50% composition, is very sharp, an indication that the predominant phase determines the continuous phase (the matrix).

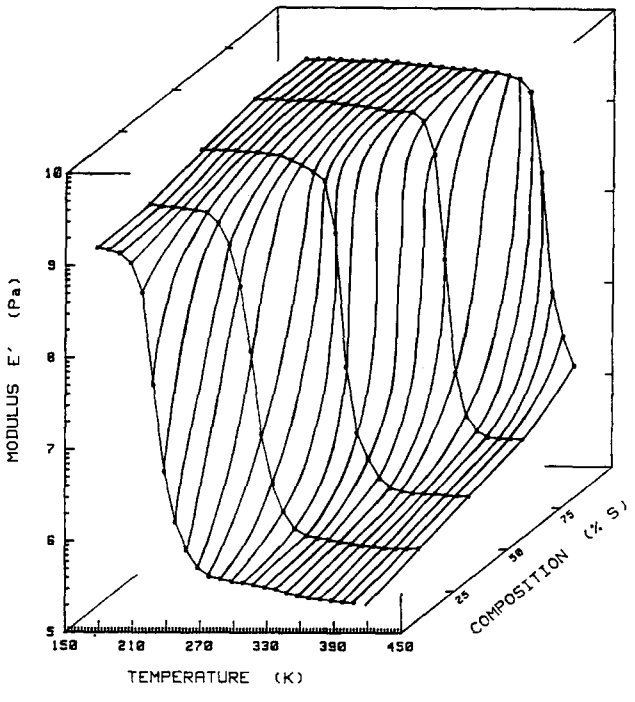

Figure 7 Three-dimensional diagram of the storage modulus *E' versus* temperature as a function of copolymer composition (S/BuA = 0/100, 25/75, 50/50, 75/25, 100/0)

Heterogeneous latex particles

Particle morphology. A preliminary morphology study of the particle structure was done prior to examining the mechanical properties of the corresponding films, whether they have core–shell or multilayered structures.

Using RuO_4 as a stain results in a darkening of the PS phase (micrograph in *Figure 9a*); in PS/S–BuA core–shell particles, the richer the styrene content in the copolymer, the more attenuated is the contrast between the two phases. In *Figure 9b*, corresponding to the CS1 sample after 10 days of film formation ageing, the particle frontiers are no longer visible due to coalescence; with the same sample, but after 30 days of ageing, a section of the film obtained by ultramicrotomy appears to be more homogeneous (*Figure 9c*).

It was found that a film formed with the multilayer latex MC1 does not reveal the layer of PBuA at the particle surface either because BuA has been polymerized within the particle (or after diffusion of the polymerized chain), or the layer thickness is too thin to be detected.

Thermomechanical properties and simulation. It is noteworthy that the morphological analysis of latex films

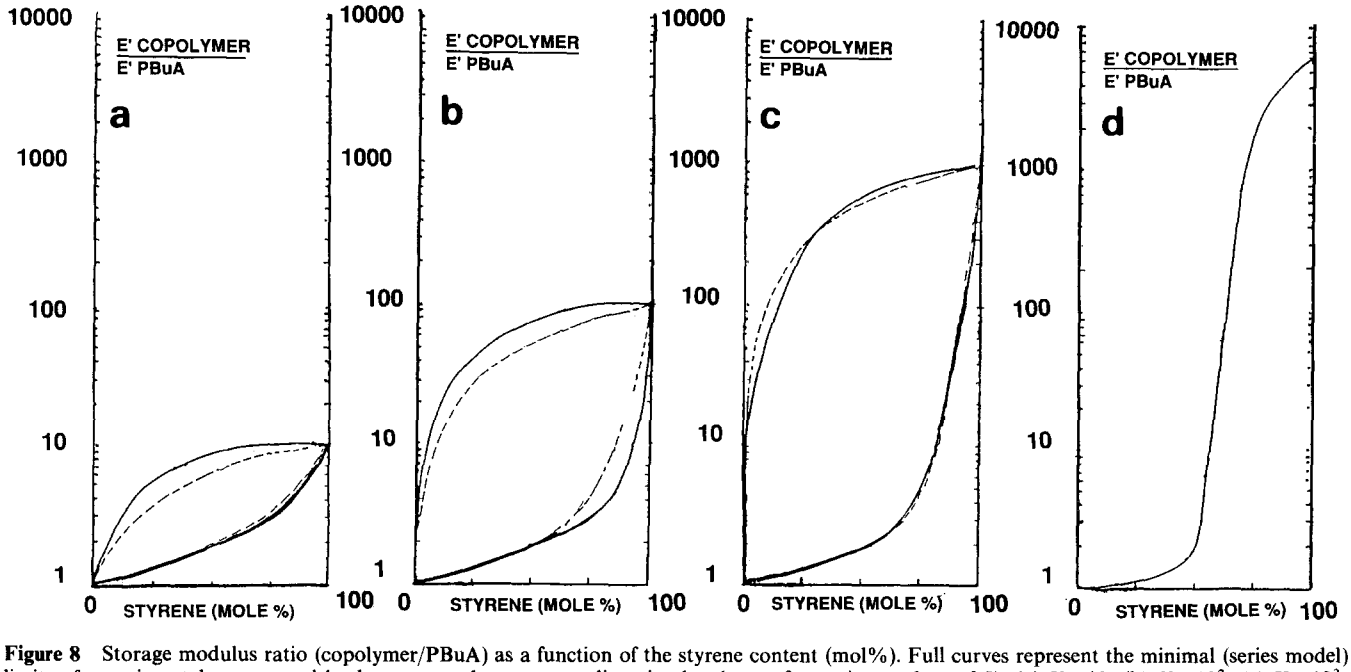

Figure 8 Storage modulus ratio (copolymer/PBuA) as a function of the styrene content (mol%). Full curves represent the minimal (series model) limits of experimental curves, and broken curves the corresponding simulated ones for various values of K: (a) $K = 10$; (b) $K = 10^2$; (c) $K = 10^3$; (d) $K = 7 \times 10^3$

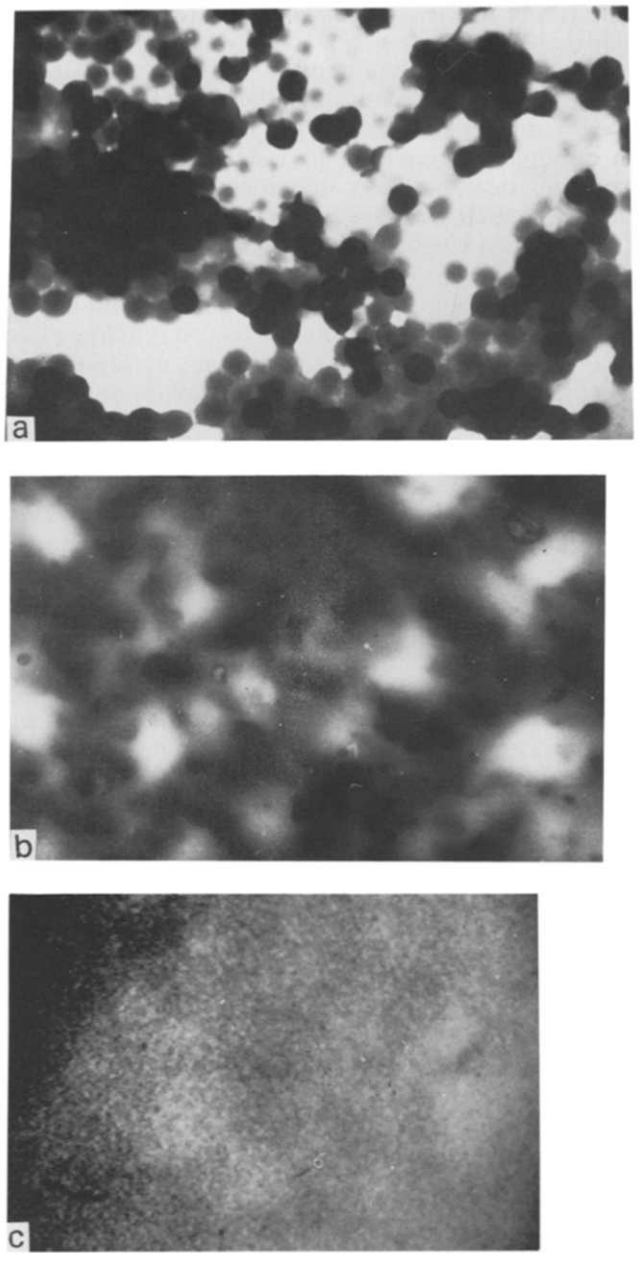

Figure 9 Electron transmission micrographs: (a) blend of two latexes, PS and PBuA, stained with RuO_4 vapour; (b) CS1 sample (S/BuA = 25/75) after 10 days of film formation; (c) ultramicrotomed section of the same film after 30 days of ageing

by transmission electron microscopy is really tricky; hence any quantitative estimation is not conceivable. On the contrary, the analysis of their mechanical properties (and comparison with the corresponding simulated ones) should provide information on this morphology.

Core–shell latex particles. One should remember that the two-phase films are formed of inclusions (PS seed) in a matrix (comprising a small amount copolymer-like material resulting from the interdiffusion of the particle shells). Results for the latex films referred to as CS2 and CS3 are reported respectively in *Figures 10* and *11* for the storage modulus variation *versus* temperature and in *Figures 12* and *13* for the damping ($\tan\delta$). Simulation curves are also given on the same diagrams; it is assumed that the 'simulated' material is made with 10 mole % PS plus 90% copolymer, the thermomechanical properties of which are well established owing to the basic relationship (8). There is good agreement between the experimental data and the theory except in the extreme domains; there, contrary to the simulated curves, the experimental ones (*Figures 10* and *11*) do not practically exhibit any rubbery domain. This discrepancy is probably due to an effect of molecular weight. As reported in *Table 2*, these molecular weights are low, as expected for copolymers prepared with a semi-continuous process, in comparison with those of polymers obtained with the corrected-batch process. In the latter case, the rubber plateau is well defined since the molecular weights are higher (*Figure 4*). The observed differences between the experimental and simulated moduli in the low-temperature domain are due to an underestimation of the copolymer properties used in the computation.

Effect of thermal annealing. The latex films were annealed at 140°C for 1 h to provide a stable equilibrium of the various phases. As illustrated in curve D of *Figure 10*, no appreciable effect is detected.

Effect of film formation temperature. Such an effect on the ultimate thermomechanical properties of films is shown in *Figures 10* and *11*, respectively at 40 and 78°C

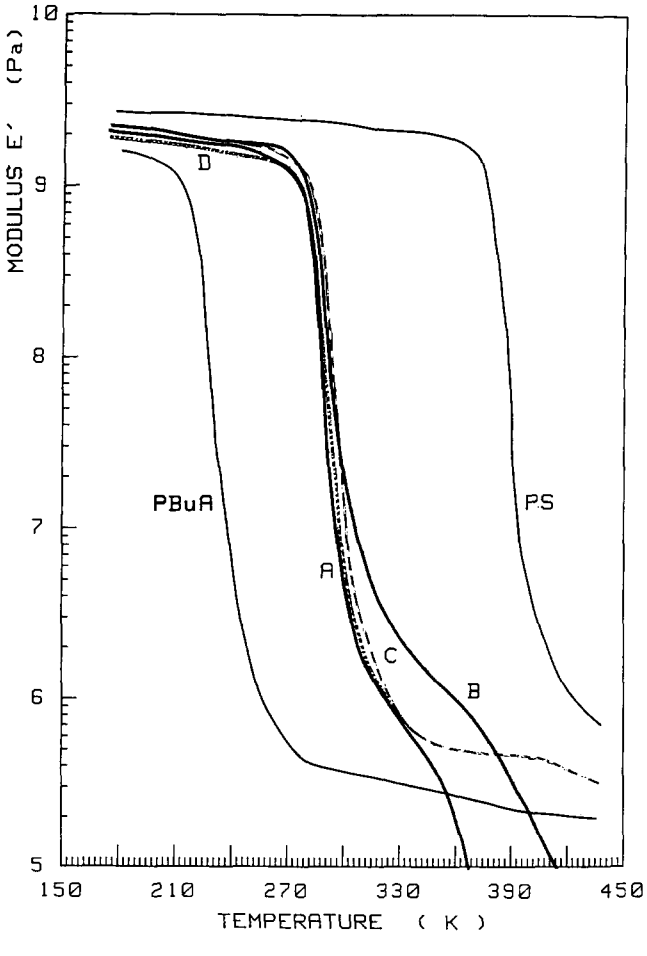

Figure 10 Storage modulus E' *versus* temperature of a film formed with latex CS2 (see *Table 1*). The figure shows experimental curves (A, B, D) and a simulated curve (C): curve A, film formed at 40°C without thermal effect; curve B, film formed at 78°C; curve C, simulation of the modulus for a composite film (10% PS seed in 90% homogeneous copolymers (S/BuA = 43/57 in mole)); curve D, film obtained at 40°C with annealing treatment at 140°C for 1 h

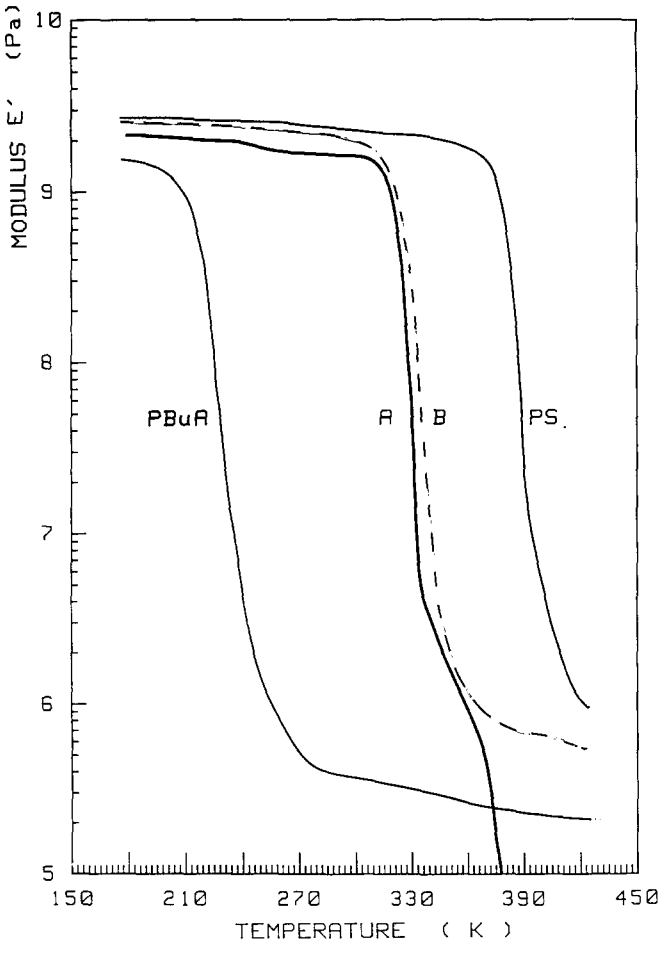

Figure 11 Storage modulus E' *versus* temperature for the latex film CS3: curve A, film obtained at 78°C; curve B, simulation of the modulus for a composite film (10% PS seed in 90% homogeneous copolymer (S/BuA = 67/33 in mole))

(curves A and B). It is found that the curves are quite similar below T_g, and more apart above T_g. It appears that the rubbery domain for the sample formed at 80°C is more pronounced than that prepared at 40°C. This difference can be interpreted by considering that particle coalescence and interdiffusion of the phases (core–shell) are more significant at higher temperature.

The same trends have been observed for the sample CS3 (in this case, the simulated curve was obtained from a material formed with inclusions (10% PS seeds) in a matrix of copolymer (composition S/BuA = 67/33 in mol%) and the same explanations can be invoked in order to explain the discrepancies between the experimental and simulated curves. The molecular-weight effect is particularly evident on the tan δ variation in the temperature domain near the PS glass transition temperature.

Films cast from multilayered latex particles. Results are reported on *Figures 14* to *17*, respectively, for samples MC2 and MC3. Concerning the sample MC2, the absence of variation for the storage modulus (or tan δ) as a function of temperature in the low-temperature range is indicative that PBuA does not exist as a pure and concentrated phase. It might be supposed that the BuA monomer can diffuse within the particles before polymerizing. This diffusion process will be more effective as the copolymer composition of the internal layers is richer in BuA. The main transition observed is in fact that of a copolymer enriched with a PBuA phase, as confirmed by the simulation (curve C). The PS phase is observed but the discrepancy between the simulated and experimental curves (*Figure 16*) is quite significant because of the molecular-weight effect. Various film morphologies have been simulated (curves B, C and D in *Figures 14* and *16*) so as to show that the proposed simulation allows a correct approach of the film structure, although the theory was roughly established.

Concerning the sample MC3 (*Figures 15* and *17*), which is a S-rich copolymer, a slight variation is seen of the modulus and tan δ in the temperature range near the theoretical T_g of PBuA (−50°C). In this case, BuA diffusion within the particles would have been less important than previously reported, since the internal layers exhibit higher T_g. The simulation (curves C and B) shows that the matrix of the film is the copolymer (which represents 80% of the total material) with two types of inclusions (PBuA and PS). There is no detectable phase due to the PS seed in the damping diagram. As already indicated, low molecular weights for these materials result in an undetectable rubbery plateau.

CONCLUSIONS

In this study, the thermomechanical behaviour of films originated from S–BuA copolymer latexes prepared by emulsion polymerization was investigated. Different pro-

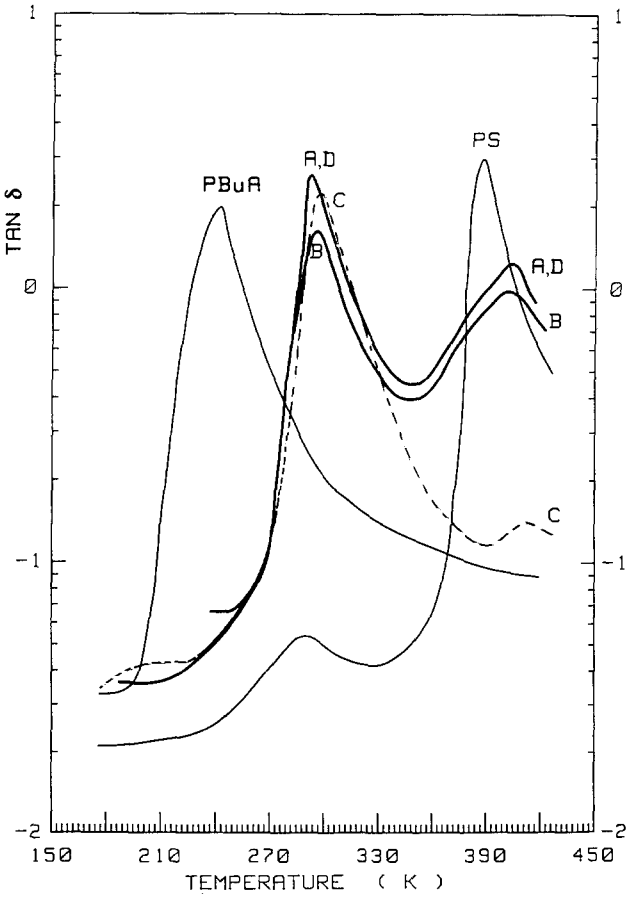

Figure 12 Tan δ *versus* temperature for the latex film CS2 (see *Figure* 10 for legend)

cesses were carried out so as to obtain various particle morphologies with three different overall S–BuA molar compositions: 25/75, 50/50, 75/25. The corrected batch process was performed in view of preparing homogeneous materials with 'ideal' microstructure. The two-stage process allowed one to get core–shell or multilayered particle latexes. With the first series of copolymers, the mechanical behaviour *versus* composition was modelled with a linear law. Then, the similarity between a two-phase composite and a homogeneous copolymer was evident, at a molecular level. It was found that a dissymmetry in the sequence distribution of the chain was reflected in a change of the damping peak (tan δ) as a function of temperature.

The thermomechanical analysis of the films issued from the coalescence of structured latex particles is indicative that two- or three-phase films do exist. The simulation of the experimental data was found to give the nature and composition of the matrix and inclusion phases. A

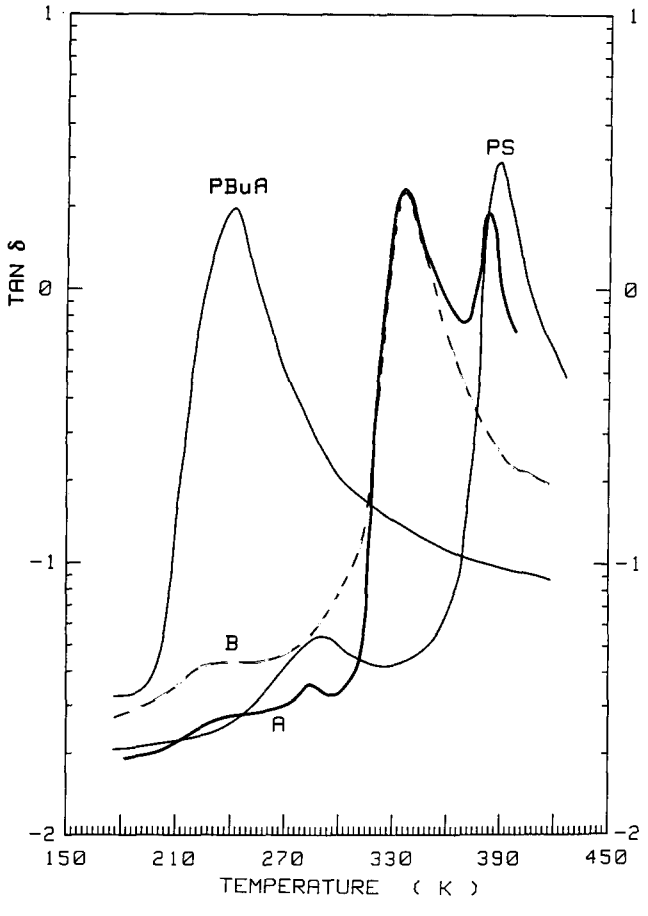

Figure 13 Tan δ *versus* temperature for the latex film CS3 (see *Figure 11* for legend)

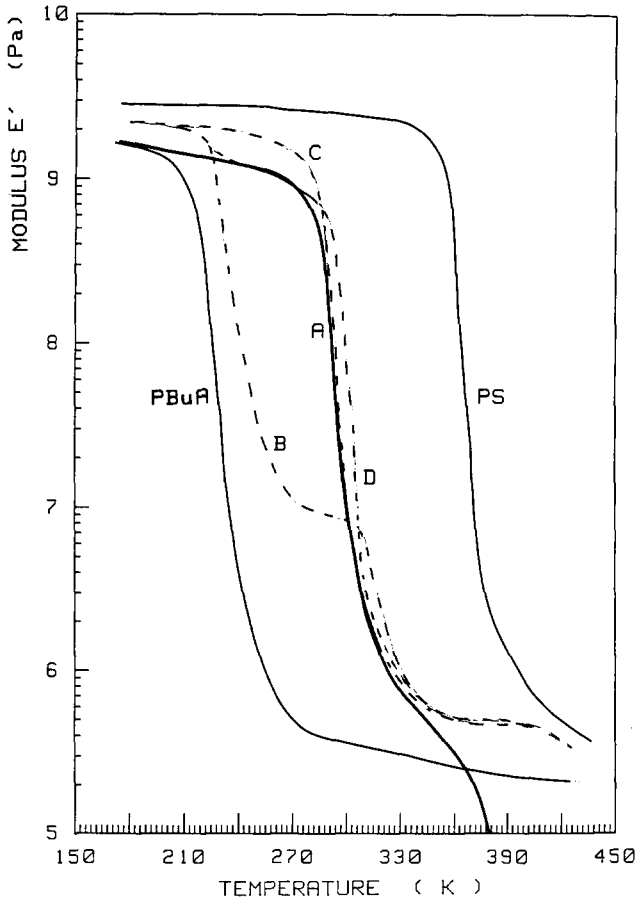

Figure 14 Storage modulus E' *versus* temperature for the latex film MC2: curve A, film obtained at 40°C (experimental); curve B, simulation of a composite film comprising composite inclusions (10% S seed occluded in 80% homogeneous copolymer (50/50)) and matrix (10% PBuA); curve C, composite inclusions (10% PS seed occluded in 10% PBuA) and matrix (80% homogeneous copolymer (S/BuA = 50/50 in mole)); curve D, 10% PS seed occluded in 90% homogeneous copolymer (S/BuA = 50/50 in mole)

Table 2 Molecular and colloidal characteristics of latexes

Latex code	Molecular weight ($\times 10^{-3}$) $\bar{M}_n$	$\bar{M}_w$	$\bar{M}_w/\bar{M}_n$	Particle diameter (Å)	Particle number ($\times 10^{-14}$ cm^{-3})
PS (seed)	355	1180	3.3	600	8.3
PBuA	not analysed		(microgels and $M_n > 10^6$)	1400	–
BC1	716	2430	3.4	930	5.1
BC2	241	1300	5.4	970	3.8
BC3	384	1726	4.5	990	5.3
CS1	80	830	10.0	990	4.5
CS2	112	885	8.0	1040	4.8
CS3	85	610	6.9	1090	3.1
MC1	(44)	467	10.6	1040	3.6
MC2	115	610	5.5	1100	3.0
MC3	115	858	7.5	1170	2.5

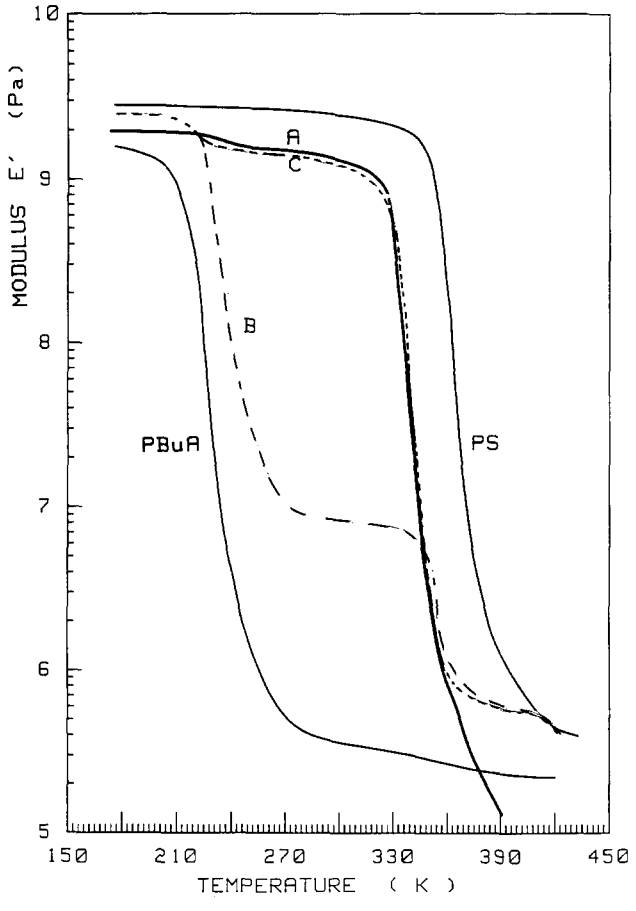

Figure 15 Storage modulus E' *versus* temperature of the latex films MC3: curve A, film obtained at 78°C (experimental); curve B, simulation of a composite film comprising 10% PS occluded in 80% homogeneous copolymer (S/BuA = 70/30 in mole) and a matrix of PBuA (10%); curve C, 10% PS occluded in 10% PBuA and a matrix of 80% of a homogeneous film (S/BuA = 70/30 in mole)

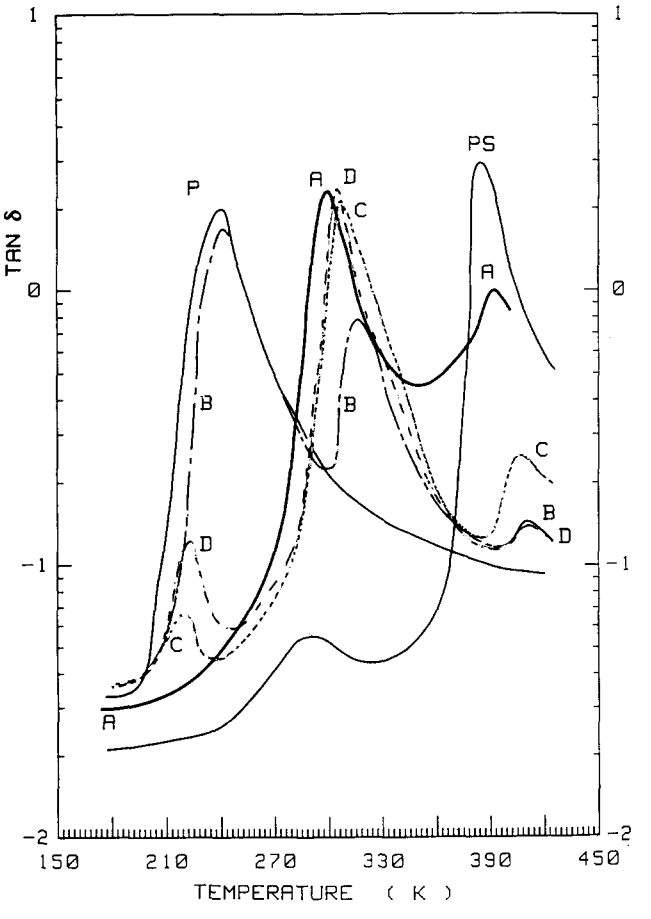

Figure 16 Tan δ *versus* temperature for the latex film MC2 (see *Figure 14* for legend)

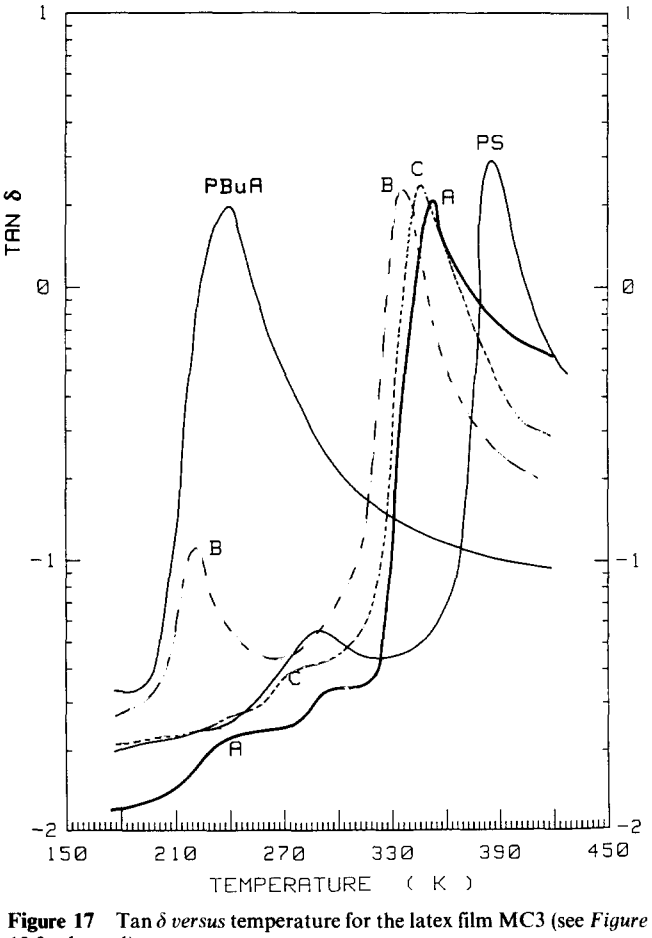

Figure 17 Tan δ *versus* temperature for the latex film MC3 (see *Figure 15* for legend)

self-consistent composite model was used, based on Kerner's equation adapted by Dickie for a strain model (dynamic stress). Core–shell and multilayered latexes lead, after coalescence, to composite films in which the PS phases (and PBuA in some cases) are occluded in a homogeneous copolymer phase. Polymer prepared with a semi-continuous process exhibits a low molecular weight, which causes the rubbery plateau to be unobservable.

From this work, it is pointed out that the simulation of the thermomechanical properties of a polymer–polymer composite from knowledge of the properties of the pure phases appears to be an interesting phenomenological approach to the coalescence of structured particles. It builds up a very useful tool, which is more suitable for determining the film morphology than for deriving information about the structure of the original latex particles.

REFERENCES

1 Daniel, J. C. *Makromol. Chem. Suppl.* 1985, **10/11**, 359
2 Hashin, Z. *J. Appl. Mech.* 1983, **50**, 481
3 Nielsen, L. E. *J. Compos. Mater.* 1967, **1**, 100
4 Cruz-Rivera, A., Rios-Guerrero, L., Monnet, C., Schlund, B., Guillot, J. and Pichot, C. *Polymer* 1989, **30**, 1872
5 Hashin, Z. Proc. 4th Int. Congr. Rheol. (Ed. E. H. Lee), Interscience, New York, 1965, Vol. 3, p. 30
6 Nielsen, L. E. *J. Compos. Mater.* 1968, **2**, 120
7 Tsai, S. W. and Hahn, H. T. 'Introduction to Composite Materials', Technomic, Stanford, Conn., 1980

8 Takayanagi, M. and Harima, H. *Am. Chem. Soc., Div. Coatings Plast. Coatings Plast. Chem., Preprints* 1963, **23**(2), 75
9 Kaplan, D. and Tschoegl, N. W. *Polym. Eng. Sci.* 1974, **14**, 43
10 Takayanagi, M., Uemura, S. and Minami, S. *J. Polym. Sci. (C)* 1964, **5**, 113
11 Horino, T., Ogawa, Y., Soen, T. and Kawai, H. *J. Appl. Polym. Sci.* 1965, **9**, 2261
12 Okamoto, T. and Takayanagi, M. *J. Polym. Sci. (C)* 1968, **23**, 597
13 Dickie, R. A. *J. Appl. Polym. Sci.* 1973, **17**, 45
14 Kraus, G. and Rollman, K. W. *ACS Adv. Chem. Ser.* 1971, **99**, 189, American Chemical Society, Washington, DC
15 Fujino, K., Ogawa, Y. and Kawai, H. *J. Appl. Polym. Sci.* 1964, **8**, 2147
16 Sperling, L. H., Taylor, D. W., Kirkpatrick, M. L., George, H. F. and Bdarman, D. R. *J. Appl. Polym. Sci.* 1970, **14**, 73
17 Dickie, R. A. and Cheung, M. F. *J. Appl. Polym. Sci.* 1973, **17**, 79
18 Kerner, E. H. *Proc. Phys. Soc. (B)* 1956, **69**, 808
19 Nielsen, L. E. *J. Appl. Polym. Sci., Appl. Polym. Symp.* 1969, **12**, 249; *J. Appl. Phys.* 1970, **41**, 4626; *J. Appl. Polym. Sci.* 1970, **14**, 1449
20 Nielsen, L. E. *Rheol. Acta* 1974, **13**, 86
21 Dickie, R. A. 'Polymer Blends' (Eds. D. R. Paul and S. Newman), Academic Press, New York, 1978, Vol. 1, Ch. 8, p. 357
22 Ashton, J. E., Halpin, J. C. and Petit, P. H. Technomic, Stanford, Conn., 1969
23 Diamant, J., Soong, D. S. and Williams, M. C. 'Contemporary Topics in Polymer Science' (Eds. W. J. Barley and T. I. Tsuraka), Plenum, New York, 1981, Vol. 4, pp. 599–627
24 Paul, B. *Trans. AIME* 1960, **218**, 36
25 Hashin, Z. *J. Appl. Mech.* 1962, **29**, 143
26 Hashin, Z. and Strikman, S. *J. Mech. Phys. Solids* 1963, **11**, 127
27 Christensen, R. M. *J. Mech. Phys. Solids* 1969, **17**, 23
28 Theocaris, P. S. *Kolloid Z.* 1969, **235**, 1182
29 Christensen, R. M. *J. Mech. Phys. Solids* 1969, **27**, 315
30 Guyot, A., Guillot, J., Pichot, C. and Rios, L. *ACS Symp. Ser.* 1981, **165**, 415
31 Guillaume, J., Essadam, H., Graillat, C., Pichot, C., Guillot, J. and Guyot, A. ACS Meeting, Polymer Preprints, Miami, 1985, Vol. 52, p. 309
32 Vanderhoff, J. W. in 'Future Directions in Polymer Colloids' in NATO Advanced Research Workshop, Racine, Wisc., 1986
33 Stutman, D. R. Klein, A., El Aasser, M. S. and Vanderhoff, J. W. *Ind. Eng. Chem., Prod. Res. Dev.* 1985, **24**, 3
34 Kato, K. *Kolloid Z.Z. Polym.* 1967, **220**(1), 24; *Polymer* 1967, **8**, 33
35 Cho, I., and Lee, K.W. *J. Appl. Polym. Sci.* 1985, **30**, 1903
36 Trent, J. S., Scheinbeim, J. I. and Couchman, P. R. *Macromolecules* 1983, **16**(4), 589
37 Nielsen, L. E. 'Mechanical Properties of Polymers and Composites', Vol. 1, Ch. 4, 1962 p. 215
38 Llauro-Darricades, M. F., Pichot, C., Guillot, J., Rios, L., Cruz, A. and Guzman, C. *Polymer* 1986, **27**, 889
39 Guillot, J. and Ramirez, W. IUPAC Symp. 170, Genoa, 1987
40 Lambla, M., Schlund, B., Lazarus, E. and Pith, T. *Makromol. Chem. Suppl.* 1985, **10/11**, 463